Effect of Oxalate on The Growth of Cuprous Oxide Layers on Copper Electrodes. Ellipsometric and Isoelectric Point Study

Jorge O. Zerbino,[1,*] **Rosa M. Torres Sánchez**[2] **and Marija G. Sustersic**[3]

[1] *Instituto de Investigaciones Fisicoquimicas Teóricas y Aplicadas (INIFTA), UNLP, Sucursal 4, C.C. 16, (1900) La Plata (Argentina)*

[2] *Centro de Tecnología de Recursos Minerales y Cerámica. CETMIC. CIC. C.C. 49, (1987) M. B. Gonnet- (Argentina)*

[3] *Faultad de Ingeniería. FICES .UNSL. 25 de Mayo 384 (5730) Villa Mercedes, San Luis (Argentina)*

* *Corresponding author: E-mail: jzerbino @inifta.unlp.edu.ar*

Dedicated to Professor Josef Barthel on the occasion of his 80th birthday

Abstract

The effect of the addition of oxalate to the growth of a cuprous oxide layer on copper electrodes was analysed at potential near that of the open circuit, in borax solutions ($7 < pH < 9$) by cyclic voltammetry, ellipsometry and surface charge techniques. The oxide formation is explained as a sequence of Cu_2O layer growth, *ippl,* cationic defect accumulation and Cu(II) adsorption on the oxide/solution interface, and a dissolution/precipitation step similar to the mechanism previously reported in oxalate free solutions. The oxalate adsorption at $pH = 9$ increases the dissolution rate and a greater thickness of the outer layer, *oppl,* is obtained. Nevertheless, the oxalate adsorption at $pH = 7$ decreases the cationic defect on the cuprous oxide/electrolyte interface, promoting the Cu_2O growth. For copper particles immersed in solutions of pH between 7 and 9, the measured isoelectric point values, *iep,* ($11.8 < iep < 11.5$) shifts in the presence of oxalate to pH between 11.6 and 11.0, respectively. This shift in the *iep* to a lower pH value indicates oxalate adsorption on the Cu/Cu_2O particles.

Keywords: Copper oxide, oxalate, ellipsometry, isoelectric point.

1. Introduction

Cuprous oxide layers have been widely studied during the last half century and it is the object of continuous attention in many technological areas such as catalysis, corrosion and electronic and photonic devices. This low cost and non-toxic semiconductor plays a critical role in the development of sensors, electroless copper plating baths, fuel cells, and photocatalytic material for splitting water into H_2 and O_2 via visible light irradiation.[1–5] The long held consensus is that the best approach to improve cell efficiency in Cu_2O-based photovoltaic devices is to achieve both *p*-type and *n*-type cuprous oxides and thus *p-n* homojunctions. Both metallic and ionic copper take part in the selective production of methane, ethylene and alcohols, although the role of the different copper oxidation states is still in discussion.[6–7]

The passivity and corrosion of copper electrodes depend on a dense and adherent oxide film, which inhibits corrosion in aqueous solutions. The passive film present a complex structure in which Cu_2O, CuO or $Cu(OH)_2$ layers are present.[6–7] The structure and the thickness of both the Cu_2O inner part of the passive layer, *ippl,* and the outer $Cu(OH)_2$ layer, *oppl,* depend on the electrode potential, the solution pH and the presence of different ions (SO_4^{-2}, CO_3^{-2}), dissolved gases (O_2, O_3, SO_2, CO) and the presence of inhibitors in the electrolyte.[2,6–8]

Cu_2O is a semiconductor that shows a variable electrochemical and optical behaviour because of the deviations in the stoichiometry of the cationic vacancies arising from its preparation methods or environmental conditions.[8–10]

Oxalic acid is a carboxylic bidentate complexing agent used to remove rust from automobile radiators, steam boilers and leaching of several metals.[11–12] Oxalate Copper (II) complexes have more high stability constant than those formed with Ni, Cr, Pb, Zn, Cd, and Fe. Different coating and modified copper electrodes are prepared with oxalate and it is used as a complexing agent in Cu and chemical mechanical planarisation.[11,13–14]

In this work, cyclic voltammetry and ellipsometric measurements are made on massive Cu electrodes to analyse the effect of oxalate addition and to characterise the interface structure with and without oxalate. Comparative isoelectric point experiments on Cu microparticles in aqueous solutions in the 7 < pH < 9 range are also presented.

2. Experimental

The experimental set-up has previously been described.[6–7,9–10] The measurements were doing in borax buffer solutions of pH = 9.0 ($Na_2B_4O_7$ 0.75 M, H_3BO_3 0.15 M), a_1 solution, and pH = 7.4 ($Na_2B_4O_7$ 0.005 M, H_3BO_3 0.18 M) b_1 solution. Solutions a_2 and b_2 were prepared by the addition of 5 mM $H_2C_2O_4$ to a_1 and b_1 solutions respectively. The pH values were adjusted by NaOH addition. All experiments were performed under N_2 bubbling, at room temperature and using hydrogen reference electrode in the same electrolyte *(RHE)*. The electrode was made by axially fitting a polycrystalline copper rod (99.99% purity) into a Teflon sheath. It was polished to a mirror finish with alumina of 1, 0.3 and 0.05 μm.

2. 1. Ellipsometric Measurements

The electrode was illuminated with monochromatic light in a visible wavelength range (400 nm < λ < 700 nm) with an incident angle of 70°. Optical data were obtained by interposing filters corresponding to five λ (405, 450, 492, 546 and 580 nm). The sampled ellipsometric area of the electrode, horizontally placed in the cell, was about one mm^2 and the electrode geometric area was 0.4 cm^2.

The freshly polished Cu electrode placed in the cell attains a rest potential E_{oc} of about 0.6 V *(RHE)* after a few minutes.[6–7] The ellipsometric parameters corresponding to the bare metal were obtained after maintaining the electrode potential during 2 min at E_c = –0.320 V *vs. RHE*. The ellipsometric parameters Δ and ψ, were recorded as a function of the potential, E, and of the time τ. The potential was scanned from E_c up to E_a at a sweep rate v = 0.5 mV s^{-1} followed by a potential holding at E_a = 0.61

V during a time τ = 60 min. Then, a cathodic scan from E_a up to E_c was performing.

2. 2. Transport Number Measurements

The isoelectric point (*iep*) measurements were done with copper powder (Arqimex, Wolstenholme, http://www.arqimex.com.ar) of a mean particle diameter in the range of 8.5–10.5 microns. Before each experiment, the powder was washed two times with acetone, and two times with 50% acetone/ water solutions and centrifuged every time at 4000 rpm, to eliminate the covering waxy stearate layer.[6–15] The *iep* determinations were performed by means of the diffusion potential measurement, from which the transport number (t^+) value was obtained in the same way as described elsewhere.[16–19]

3. Results and Discussion

3. 1. Voltammetric and Ellipsometric Measurements

Fig. 1 shows the evolution of the ellipsometric parameters Δ and ψ corresponding to the copper electrode at pH = 9 in the solution with (a_2) and without oxalate (a_1),
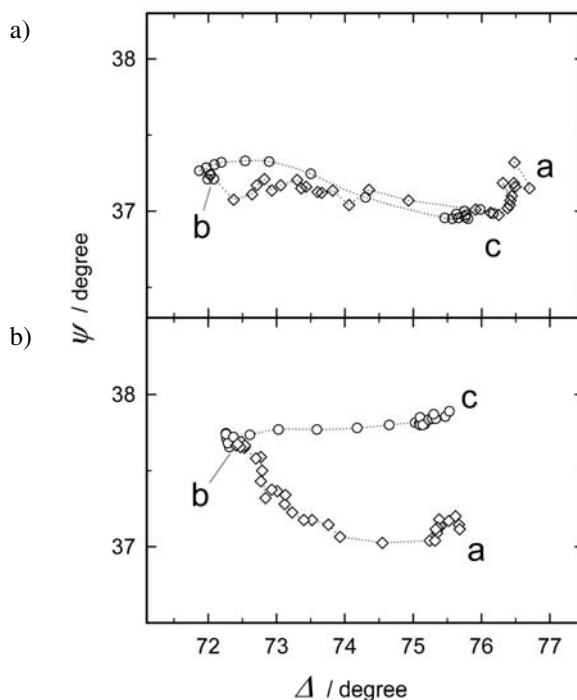

Figure 1. Comparison of Δ and ψ values measured at pH 9.0 during a cycled scan at v = 0.5 mV/s between E_c –0.31 V and E_a = 0.61 V, followed by potential holding at E_a for τ = 60 min. (a) without and (b) with $(C_2O_4)Na_2$ 5 mM. ($\diamond$) anodic scan and potential holding at E_a, ($\bigcirc$) cathodic scan. (a) bare electrode, (b) τ = 60 min., (c) E_c = –0.31 V.
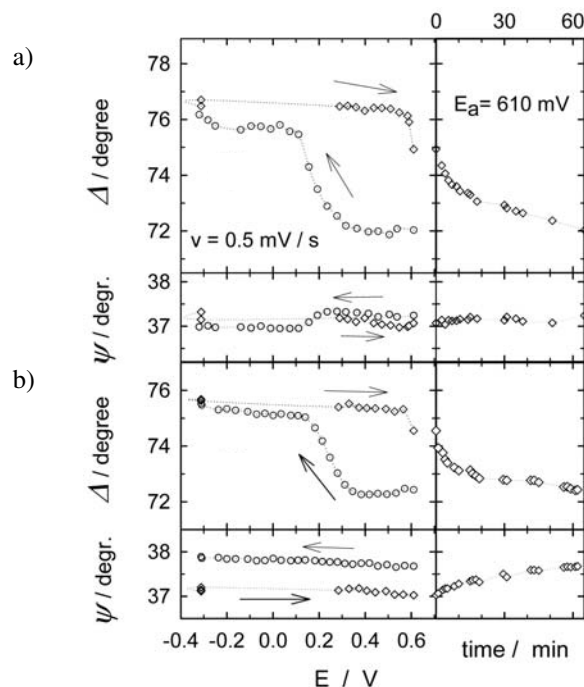
a)

Figure 2. The same experiment of Fig.1 but as a function of potential *E* (left side) and holding time *τ* at *E*$_a$ = 0.61 V (right side). (a) without and (b) with (C$_2$O$_4$)Na$_2$ 5 mM, pH 9.0. (◇) anodic scan and potential holding at *E*$_a$, (○) cathodic scan.

during a cycling in the potential region between *E*$_c$ = –0.32 V and *E*$_a$ = 0.610 V at *v* = 0.5 mV s^{-1}. The same data was plotted as a function of the electrode potential and the holding time at *E*$_a$ = 0.610 V: *Δ* / *E*, *ψ* / *E*, *Δ* / *τ*, *ψ* / *τ*, (Figure 2).

In both solutions, at potentials higher than 0.55 V, *Δ* variation, –*δΔ* increases. In the solution without oxalate, with *τ* > 10 min., –*δΔ* increases linearly with *τ*. Nevertheless *ψ* remains practically constant during all the experiment. On the other hand, in solutions containing oxalate the –*δΔ* increase at *τ* > 10 min is comparatively lower and an irreversible increase of *ψ* is noticed during the holding at *E*$_a$ = 0.610 V. *ψ* remains invariable during the next cathodic scan.

Previous experiments showed that the *oppl* thickness might increase when high anodic potentials and long holding times are applied and it grows during the cathodic reduction of the *ippl*.[6–7,10,20] The observed increase of *ψ* during the potential holding in *a$_2$* solution indicates the growth of a lesser dense and more thick layer, *oppl*, that corresponds to a very hydrated Cu(OH)$_2$. This less compact hydrated layer is not electroreduced at cathodic potentials.

At pH ≈ 9 copper shows the highest stability and the maximum precipitation of the dissolved substances. Previously reported results show that a Cu/ Cu$_2$O/ Cu(OH)$_2$ · xH$_2$O double layer grows under anodisation. A Cu$_2$O dehydrated layer adjacent to the metal (*ippl*) and an

outer hydrated layer (*oppl*).[6–7,10,20] The Cu$_2$O stoichiometry, the number of carriers and the thickness of the two parts of the passive layer depend strongly on the pH, electrolyte composition and the applied anodisation programme.[21]

For thinner films –*δΔ* can be considered as proportional to the thickness of the *ippl*. In the potential region 0.471 < *E* < 0.610 V corresponding to the redox couples Cu/ Cu$_2$O and Cu/CuO a linear dependence of –*δΔ* with *E* and *τ* is obtained. At *E* > 0.61 V the linear *δΔ* / *E* law attains a limit thickness. At *E* ≥ 0.67 V, corresponding to the Cu$_2$O/CuO redox couple potential, a significant increase of copper dissolution and the precipitation of the *oppl* is observed. The total amount of deposited hydrated oxide, *oppl,* which is not cathodically electroreduced, can be estimated through the *ψ* change resulting after cathodic reduction.

After some min. of immersion in *a$_1$* and *b$_1$* solutions the freshly polished Cu electrode spontaneously attains an open circuit potential *E*$_{oc}$ between 0.650 < *E*$_{oc}$ < 0.680 V (vs. *RHE*) while in *a$_2$* and *b$_2$* solutions reach a lower potential of about *E*$_{oc}$ = 0.550 V.[20] This change in *E*$_{oc}$ as well as the *ψ* increase observed in the oxalate solution is in accordance with reported thermodynamic potential-pH diagrams.[11]
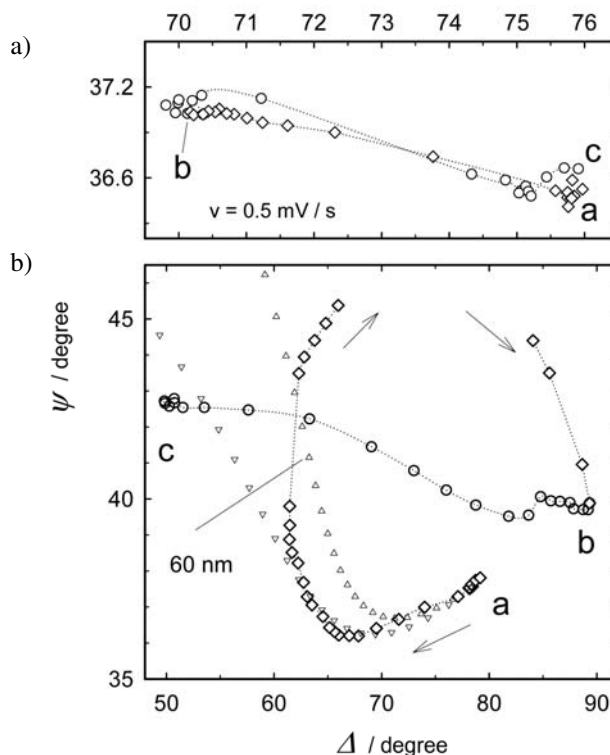
a)

b)

Figure 3. Comparison of *Δ* and *ψ* values measured at pH 7.4 during a cycled scan at *v* = 0.5 mV/s between *E*$_c$ –0.3 V and *E*$_a$ = 0.61 V, followed by potential holding at *E*$_a$ for *τ* = 60 min. (a) without and (b) with (C$_2$O$_4$)Na$_2$ 5 mM. (◇) anodic scan and potential holding at *E*$_a$, (○) cathodic scan. (a) bare electrode, (b) *τ* = 60 min., (c) *E*$_c$ = –0.31 V.
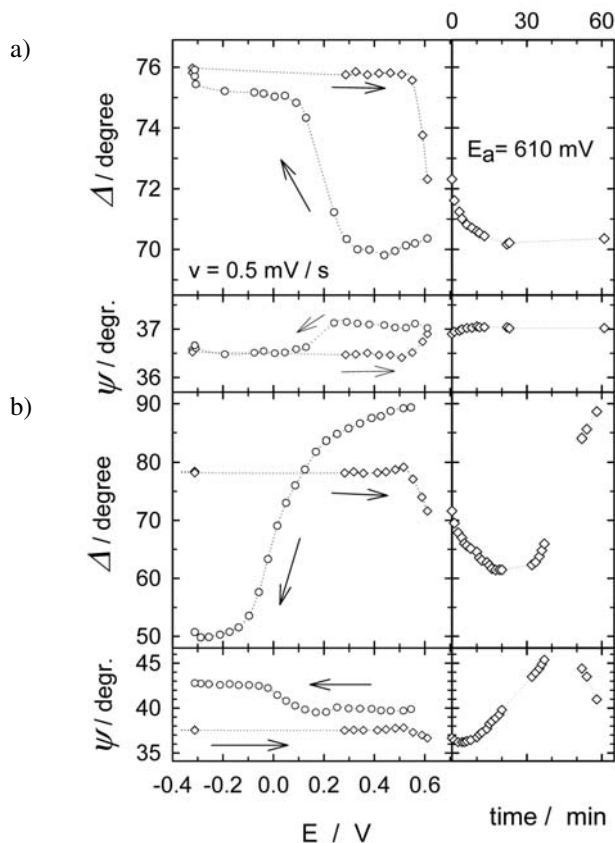
Figure 4. The same experiment of Fig.3 but as a function of the potential *E* (left side) and the holding time τ at E_a = 0.61 V (right side). (a) without and (b) with $(C_2O_4)Na_2$ 5 mM, pH 7.4. ($\diamond$) anodic scan and potential holding at E_a, ($\bigcirc$) cathodic scan.

Figs 3b and 4b. A significant and continuous change in Δ and ψ results after 10 min. of potential holding at 0.61 V in b_2 solution. After a linear decrease in Δ, that is higher than that observed in b_1 solution, rising up in the plane Δ/ψ a gradual clockwise displacement involving a change of about than 30 degree in Δ and 10 degree in ψ. After the reduction scan the resulting Δ/ψ values are very far from the initial stage corresponding to the bare surface. The Fig 4b includes also two theoretical profiles calculated chosen constant optical indexes and an increase in thickness *d*, each 4 nm.

To evaluate the structure of oxide film, *ippl,* grown during the potential holding at E_a = 0.610, a single layer model was assumed. The optical indexes $n - i\,k$ in the visible wavelength range $405 < \lambda < 580$ nm, *(n)* refraction index and *(k)* optical absorption constant, and the thickness *(d)* corresponding to the *ippl* are fitted using the Δ/ψ measurements taken at the different wavelengths. This procedure allows the univocal determination of *d*, *n* and k.[6,9–10,21] The experimental data was fitted using the gra-
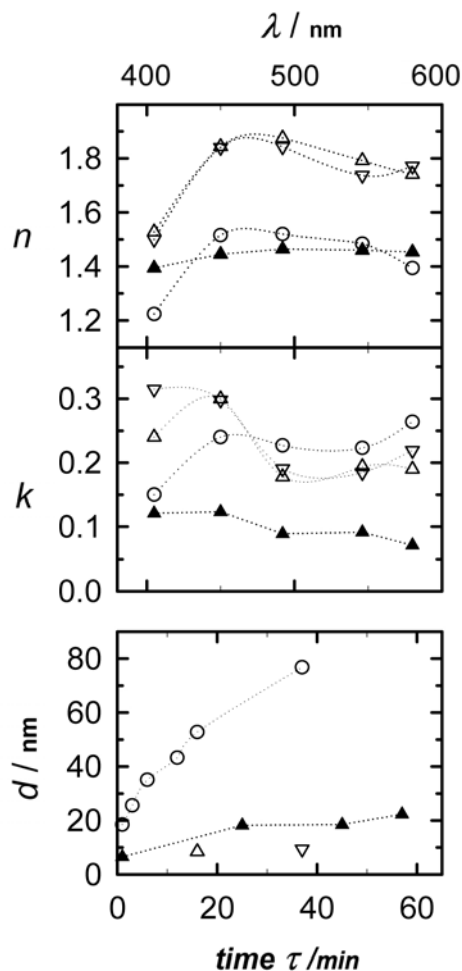
According to Pourbaix diagrams, solid cupric oxalate could form at relatively low pH and Cu^{+2} concentrations higher than 10^{-3} M. Aqueous solubility diagrams shows that $Cu(C_2O_4)$ is stable at pH values lower than 6.0 while copper oxides are stable in the higher pH region. In the calculations $Cu(OH)_2$ was not considered because it is less stable than cupric oxide. The diagrams also predict the shrinking of the CuO and Cu_2O stability regions for decreasing copper and increasing total oxalic acid concentrations.[11]

Figs. 3 and 4 show the effect of the pH on similar experiments of those described in Fig 1 and 2, namely Δ/ψ, and Δ/E, ψ/E, Δ/τ, ψ/τ, plots in solutions with and without oxalate at pH = 7.4, b_2 and b_1 solution, with E_a = 0.610 V. The Δ/ψ plot in solutions b_1 is similar to that of a_1 solution showing a reversible behaviour where the final values obtained after reduction practically coincide with those of the bare electrode. However, an increase of about 1 degree in the Δ total change as well as a variation in the Δ/ψ slope are noticed during the scan in Fig. 3a, related to that shown in Fig. 1a.

Above 0.55 V Δ continuously decreases in both solutions. However, a striking contrast is noticed comparing

Figure 5. Fitted values of *n, k* and *d*. E_a = 0.61 V. ($\blacktriangle$) pH 9.0 without $(C_2O_4)Na_2$. ($\triangle$ and $\triangledown$) pH 7.4 without $(C_2O_4)Na_2$, ($\triangle$) τ = 18 min, ($\triangledown$) τ = 38 min. ($\bigcirc$) pH 7.4 with $(C_2O_4)Na_2$ 5 mM.

dient technique and minimizing the G function.

$$G = \Sigma(\Delta_{ij}^{ex} - \Delta_{ij}^{the})^2 + (\Psi_{ij}^{ex} - \Psi_{ij}^{the})^2$$

where the subscript *i* corresponds to the optical data measured at different λ_i while the subscript *j* corresponds to different time or thickness. Δ_{ij}^{the} and Ψ_{ij}^{the} are functions of the indexes, $n_i - k_i$, and the thicknesses, d_j. The optimisation method converges, after *m* iteration, to theoretical values Δ_{ij}, Ψ_{ij}. The convergence is completed for increasing *m* when: a) the euclidean norm of the arrangement, $p_m - p_{m+1}$, tends to 0, b) $G(p_m) > G(p_{m+1}) > G(p_{m+2})$ and c) $\partial G_m / \partial p$ tends to 0.

The optical indexes plotted in Fig 5 correspond to the layer growth at pH 9 show lower *n* and *k* values than those corresponding to pH 7.4. On the other hand the thickness *d* is higher at pH 9. This indicates a more hydrated or porous *ippl* at pH 9 than at pH 7.4.

Cu$_2$O is reported to have high transparency, with a slightly yellowish appearance. It usually absorbs at wavelengths below 600 nm, whilst CuO absorbs strongly throughout the visible spectrum and is black in appearance.[8,22] The decrease in absorbance of Cu$_2$O bellow 450 nm indicates an increase in cationic defect or a higher contribution of the fase CuO$_{0.67}$.[22] The *k* values of the very thin and compact layer grow at pH 7.4, b_1 solution, indicate higher cationic defect for lower holding times ($\tau = 18$min) and also a little thickness increase with the holding time (d ≈ 8.4 and 9.4 nm for $\tau = 18$ and 38 min, respectively).

The fast growth of the oxide layer is promoted at pH 7.4 (b_2 solution) if the oxalate is present. The optical index *n* is similar to that obtained in pH 9 solutions, indicating that the oxide layer in b_2 solution is optically less dense than that in the b_1 solution.

3. 2. Isoelectric Point Measurements

Through *iep* measurements the diffuse layer variations of copper particles after immersion in pH 7.4 and 9 solutions with and without oxalate addition are investigated. The *iep* value can be determined by the transport number t^+ *vs.* pH curve and corresponds to the pH when both cations and anions in the sample have equal mobility, this happened at $t^+ = 0.5$ (Fig. 6). Since the t^+ values correspond to the average mobility of all cations (adsorbed and free) contained in the sample, when amounts of free ions are 100 times lower than the adsorbed ones,[19] the calculated t^+ value is considered to correspond to the adsorbed ion (counter ion). The *iep* is defined as the pH value when the surface has no net charge. Accordingly, the particle charge in the *iep*, attributed to the copper oxide/ electrolyte diffuse layer, has no contribution and in consequence the t^+ corresponds to the transport number of the mobile K$^+$ cation. The measured *iep* match the previously reported data obtained for metallic Cu particles using different methods.[6]
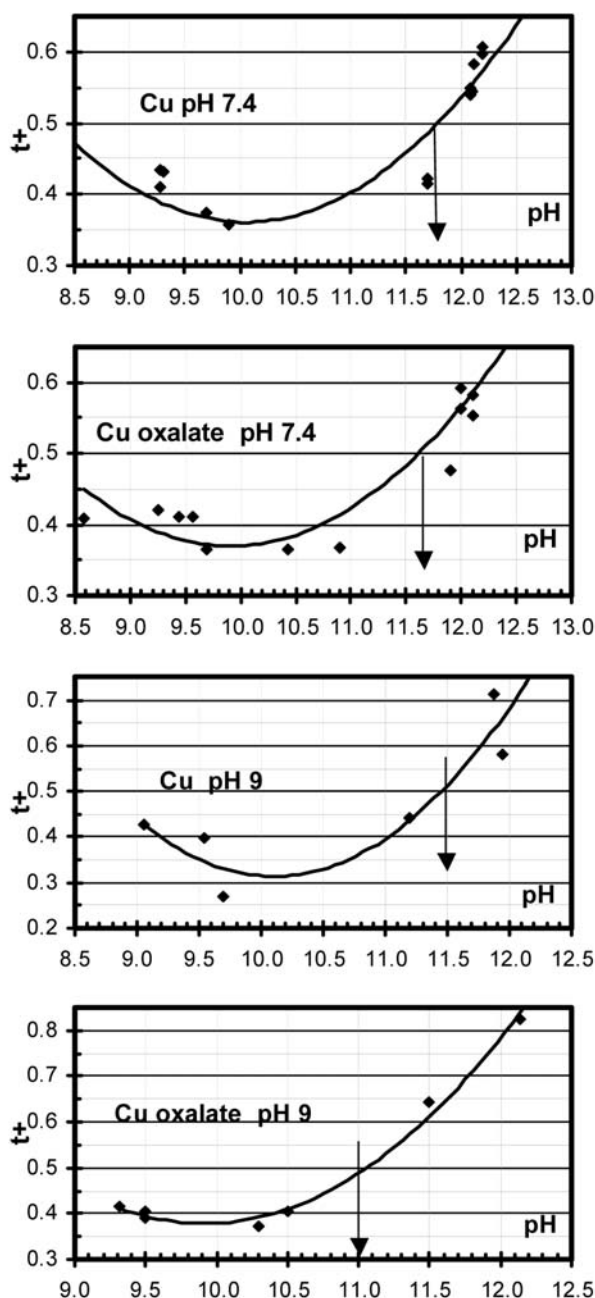

Fig. 6. Calculated transport number for copper particles immersed in 9.0 and 7.4 pH solution with and without 5 mM (C$_2$O$_4$)Na$_2$.

Figure 6 shows the $t +$ vs. pH curves for Cu particles in a_1, a_2, b_1 and b_2 solutions. A decrease of around half pH unit is observed in pH 9 solutions and a lower decrease at pH 7.4 related to the value obtained in oxalate free solutions.

The oxidation of Cu to Cu$_2$O occurs by means of a hole mechanism. The flat band potential $(E_{fb})_1 \cong 0.39$ V corresponds to the potential of the couple Cu/ Cu$_2$O.[20] The region over this potential is subjected to a thickness potential linear law, *d* vs. *E*, and for anodic potentials corresponding to the Cu/CuO couple, $(E_{fb})_2 \cong 0.61$ V, a thickness limit is obser-

ved. The thickness limit may be related to a higher increase of the cation defect on the outer part of the Cu_2O layer in contact with the electrolyte or higher Cu(II) adsorption. Further CuO dissolution occurs at higher anodic potentials.

In Cu_2O the charge density near the Cu nucleus deviates substantially from spherical symmetry and the copper is linelly coordinate by two oxygen atoms. This low coordination numbers are very unusual for oxides and that is explained assuming s-d$_{z2}$ hybridisation. Such a hybridisation is rather unusual in an ionic semiconductor.[23]

The hydrated cation Cu^{+2} tend to behave as a weak acid.[24] On Cu the reported likely oxalates being Cu(Ox) and $Cu(Ox)_2^{2-}$.[5] Oxalates Copper (II) complexes have higher stability constants than other metal ions.[12,24–25] Likewise oxalate can function as a bisbidentate ligand, coordinating two metal ions and can form a wide variety of polynuclear complexes.[26] They present anisotropy and lateral interactions of either hydrophylic or strong hydrophobic nature.[27–29] Cu(I) oxalate complexes stabilised by Lewis bases are also reported.[30] Moreover, the presence of a surface in the vicinity can affect the interaction free energy of ions, modify the H-bond network and form a stable solvent-separated ion pairs.[31–32] Regarding OH electroadsorption a higher stability of $Cu_2O(111)$ related to that of $Cu_2O(001)$ is reported.[33]

Stoichiometric deviations arising from its preparation method change the number of carriers and even the *p* or *n* type character of Cu_2O. The hydrophobic nature of the copper oxide surface structure is also investigated.[8] Wetability is mainly governed by both the chemical composition and the geometrical microstructure. Increasing surface roughness of a hydrophobic material can dramatically enhance its water repellence.[4] The adsorption of oxalate on the compact cuprous oxide layer formed at pH 7.4 solutions have the effect of both, increase the anodic polarisation and reduce the cationic defect on the Cu_2O/electrolyte interface *(ippl)* leading to increasing cuprous oxide growth rate.

4. Conclusion

For pH 9 and pH 7.4 solutions, the presence of oxalate decreases the *iep* indicating oxalate adsorption on the cuprous oxide/electrolyte interface. At high pH oxalate promotes the *oppl* growth on the cuprous oxide layer formed on copper anodically polarized at $E = 0.61$ V. At the same potential but lower pH 7.4, oxalate significantly increases the thickness growth rate of the *ippl*.

5. Acknowledgements

6. References

1. R. Inguanta, S. Piazza, C. Sunseri. *Electrochem. Acta* **2008,** *53,* 6504–6512.
2. R. Pauliukaite, E. Norkus. *Acta Chim. Slov.* **2007,** *54,* 617–622.
3. M. Finsgar, I. Milosev, B. Pihlar, *Acta Chim. Slov.* **2007,** *54,* 591–597.
4. L. Wang, M. Tao. *Electrochem. Solid-State Lett.* **2007,** *10 (9),* H248–H250.
5. A. M. Fenelon, C. B. Breslin. *J. Electrochem. Soc.* **2003,** *150,* B540–546.
6. R. Torres Sánchez, A. M. Castro Luna, J. O. Zerbino. *J. Colloid Interface Sci.* **2003,** *264,* 114–120.
7. L. M. Gassa, A.M. Castro Luna, R. Torres Sánchez, J.O. Zerbino. *Portugaliae Electrochimica Acta.* **2004,** *22,* 81–91.
8. A. A. Ogwu, E. Bouquerel, O. Ademosu, S. Moh, E. Crossan, F. Placido. *Acta Materialia* **2005,** *53,* 5151–5159.
9. J. O. Zerbino. *Electrochim. Acta,.* **1999,** *45,* 819–825.
10. J. O. Zerbino, C. Tapia, R.O. Lezna. *IOM Communications.* Inst. of Mater. European Fed. of Corros. Series (EFC28) **2000,** *28,* 225–235.
11. S. Aksu. *J. Electrochem. Soc.* **2005,** *152,* G938–G943.
12. M. M. D. Jimenez, M.P.E. Gonzalez, W. Geyer, J. Mattusch, R. Wennrich. *Colloid Surface A* **2003,** 219–243.
13. V. Shinde, S.R. Sainkar and P.P. Pati. *Corrosion Sci.* **2004,** online 27 Sept. 2004,
14. C. B. Breslin, A. M. Fenelon, K. G. Connroy. *Mater. Design.* **2005,** *26,* 233.
15. S. Sheibani, A. Ataie, S.H. Manesh. *J.Alloys Comp.* **2008,** *465,* 78–82
16. R. M. Torres Sánchez, H.J. Gasalla, E.E. Pereira., *React. of Solids.* **1989,** *7,* 53–60.
17. R. M. Torres Sánchez, *J. Mater. Sci. Letters* **1996,** *15,* 461–462.
18. M. Tschapek, R. M. Torres, C. Wasowski, *Z. Pflanzenernähr. Bodenk.* **1989,** *152,* 73–76.
19. M. Tschapek, M. I. Natale, *Kolloid S. für Polymers* **1973,** *251,* 490–495.
20. J. O. Zerbino, L. M. Gassa. *J. Solid State Electrochem,* **2003,** *7,* 177–182.
21. J. O. Zerbino, M. F. L. de Mele. *J. Appl. Electrochem.* **1997,** *27,* 335–344.
22. H. Wieder, A. W. Czanderna. *J. Appl. Phys.* **1966,** *37,* 184–187.
23. P. Marksteiner, P. Blaha, K. Schwarz. Condens. Matter 1986, 64, 119–127.
24. M. Bester Rogac, V. Babic, T. M. Perger, R. Neueder, J. Barthel. *J. Mol. Liq.* **2005,** *118,* 111–118.
25. T. Tüken, G. Arslan, B. Yazici, M. Erbil. *Progr. Org. Coatings* **2004,** *49,* 153–159.

26. X. F. Chen, P. Cheng, X. Liu, B. Zhao, D. Z. Liao, S. P. Yan, Z. H. Jiang. *Inorg. Chem.* **2001**, 40, 2652–2659.

27. N. Jongen, P. Bowen, J. Lemaitre, J. C. Valmalette, H. Hofmann. *J. Colloid Interface Sci.* **2000**, 226, 189–198.

28. A. Zouaoui, O. Stephan, M. Carrier, J. C. Moutet. *J. Electroanal. Chem.* **1999**, *474*, 113–122.

29. L. C. Soare, P. Bowen, J. Lemaitre, H. Hofmann. *J. Phys. Chem. B* **2006**, *110*, 17763–17771.

30. I. Chorny, K. A. Dill, M. P. Jacobson. *J. Phys. Chem. B* **2005**, *109*, 24056–24060.

31. K. Köhler, J Eichhorn, F. Meyer, D. Gvidovic. *Organometallics* **2003**, *22*, 4426–4432.

32. N. A. Chumaevskii, M. N. Rodnikova, J. Barthel. *J. Mol. Liq.,* **2004**, *115*, 63–67.

33. J. Kunze, V. Maurice, L. H. Klein, H. H. Strehblow, P. Marcus. *Corros. Sci.* **2004**, *46*, 245–264.

34. Z. Guo, J. Fang, L. Wang, W. Liu. *Thin Solid Films* **2007**, *515*, 7190–7194.

Povzetek

Z različnimi metodami (ciklična voltametrija, elipsometrija, meritve površinskega naboja) smo raziskovali vpliv dodatka oksalata na rast plasti bakrovega oksida na bakrovih elektrodah. Sklepamo lahko, da nastanek bakrovega oksida spremlja zaporedje različnih procesov: rast Cu_2O plasti (notranji del pasivne plasti), defektna adsorpcija kationov na mejni površini oksid/raztopina ter stopnja raztapljanja/obarjanja, podobno kot v raztopinah brez prisotnega oksalata. Adsorpcija oksalata pri pH = 9 poveča hitrost raztapljanja v debelejšem delu zunanje plasti (zunanji del pasivne plasti), medtem ko pri pH = 7 zmanjša kationski defekt na vmesti plasti bakrov oksid/elektrolit kar pospešuje rast Cu_2O plasti. Izoelektrična (ie) točka bakrovih delcev v raztopini pri 7 ≤ pH ≤ 9 znaša 11.8 ≤ ie ≤ 11.5 in v prisotnosti oksalata premakne vrednost pH k 11.6 oz. 11.0, kar kaže na adsorpcijo oksalata na Cu/Cu_2O delcih.